Femtosecond Fluorescence Study of the Substitution Effect on the Proton Transfer in Thermochromic Salicylideneaniline Crystals

Taro Sekikawa and Takayoshi Kobayashi*

Department of Physics, University of Tokyo, Tokyo 113, Japan

Tamotsu Inabe

Department of Chemistry, Hokkaido University, Sapporo 060, Japan

Received: July 8, 1996; In Final Form: October 1, 1996[⊗]

The substitution effect on the dynamics of the proton transfer in thermochromic salicylideneanilines in the crystalline phase was investigated using femtosecond time-resolved fluorescence spectroscopy. From the deuteration effect and low-temperature measurement, it is concluded that the proton tunnels the potential barrier quantum-mechanically in the excited state. The rate of proton transfer was found to decrease with the energy separation between the excited enol and keto forms due to the different potential-barrier heights. The change in the potential-barrier height is qualitatively explained by the electron-donating or -accepting property of the substituent around the hydrogen bond. The thermalization of the vibrational states of the excited enol form was also observed.

I. Introduction

The photoinduced proton transfer either from one moiety to another in a molecule or between two molecules is of great interest from both basic and application viewpoints.[1−4] It is regarded as one of the simplest chemical reactions and is related to some biological processes. There have been continuing extensive arguments as to whether or not the transfer is taking place by a quantum-mechanical tunneling process.[1] In terms of application, the proton transfer might be used for optical memory or as a switch utilizing the large spectral changes induced by the configurational rearrangement of the π electrons.

Since the proton transfer changes the electronic state of a molecule, it is expected that the substituent groups near the hydrogen bond may change the potential of the proton in the hydrogen bond. Thus, the dynamics of the proton transfer strongly depends on the distribution of the π electrons around the intramolecular hydrogen bond. In the present paper, we focus on the substitution effect on the dynamics of the photoinduced proton transfer in salicylideneanilines (SAs) in the crystalline phase. Although the development of the femtosecond pulse laser makes it possible to trace the process of the proton transfer, most of the previous studies have been performed in the liquid[5−14] or in the gas phase.[15] In the liquid phase, the hydrogen-bond length might be different even in the nonpolar solvent with lack of planarity of a molecule and the viscosity of the solvent influences the proton dynamics as shown by many previous studies.[4,8,11,16−20] Thus, the investigation in the crystal phase is expected to provide information on the intrinsic dynamics of the proton.

Among the many systems with an intramolecular hydrogen bond, the thermochromic SAs in the crystalline phase[22−29] are picked in the present study. According to previous studies,[22−29] a schematic energy diagram of the thermochromic SA is considered to be the inset of Figure 1. In the ground state, the enol form is more stable than the keto form. The energy separation between these tautomers in the ground state is small enough for the keto form to be thermally populated. Thus, the absorption spectrum changes drastically with temperature. On the other hand, in the excited state, the keto form is more stable than the enol. Thus, the proton moves spontaneously to the opposite side in the hydrogen bond very rapidly by photoexcitation, which is the origin of the large Stokes shift of the fluorescence. Consequently, the thermochromic SA is considered to perform a closed reaction cycle with the enol−keto-type proton transfer by photoexcitation without *cis*−*trans*

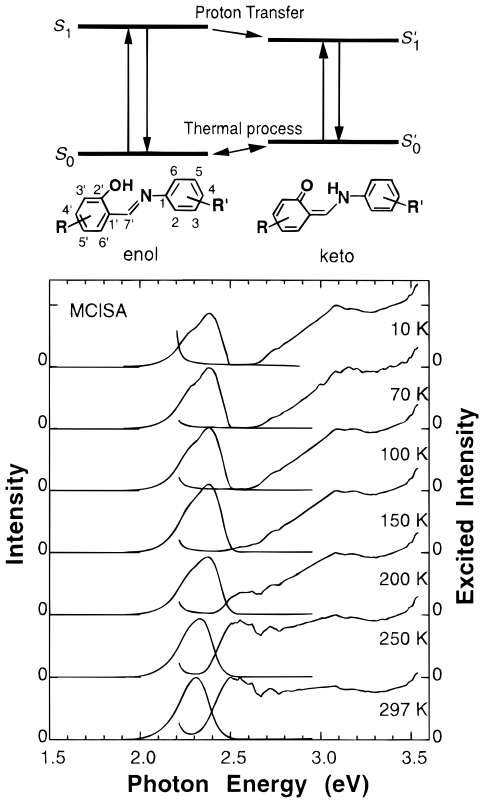

Figure 1. Stationary fluorescence and excitation spectra at various temperatures of MClSA. The excitation energy of the fluorescence spectra was 3.10 eV. The probe energy of the excitation spectra was 2.18 eV. The inset shows the energy diagram and the consitutional formulas of a thermochromic SA.

[⊗] Abstract published in *Advance ACS Abstracts,* December 15, 1996.

S1089-5639(96)02012-9 CCC: $14.00

isomerization, unlike the photochromic SA.[16,30−35] It is known that the thermochromic and the photochromic properties are exclusive in SAs.[22] The difference between the thermochromic SAs and photochromic ones is in the crystal structure: Since the photochromic SAs are nonplanar and have rather loosely packed crystals, the *cis*−*trans* isomerization can be caused by photoexcitation.[23,24]

In order to reveal the substitution effects, three thermochromic SAs were investigated: (1) *N*-5′-chlorosalicylideneaniline (ClSA), (2) 4-methyl-*N*-5′-chlorosalicylideneaniline (MClSA), and (3) 4-methyl-*N*-salicylideneaniline (MSA). The comparison among these three samples is expected to reveal the substitution effects on the dynamics of the proton transfer.

In the present paper, we have measured the lifetimes of the excited enol states of the thermochromic SAs, which are determined by the proton-transfer time, using femtosecond fluorescence spectroscopy.[36] The rate of proton transfer was found to change drastically by the substitution. The change in the proton dynamics is attributed to the different barrier heights of the proton potential in the excited state. The effect of the substituent is discussed in terms of electronic theory.

II. Experiment

ClSA, MClSA, and MSA were prepared by the condensation of chlorosalicylaldehyde and aniline, by the condensation of chlorosalicylaldehyde and *p*-methylaniline, and by the condensation of salicylaldehyde and *p*-methylaniline in refluxed methanol, respectively. Single crystals of these samples were grown from the methanol solution by slow evaporation.

The steady-state fluorescence and excitation spectra were measured by a spectrofluorometer. The light source was a Xe lamp. All excitation spectra were corrected for the intensity of the light source using a thermopile. A continuous liquid He flow cryostat was used to measure the fluorescence and excitation spectra at various temperatures.

The fluorescence decay in the femtosecond region was measured using a femtosecond fluorescence up-conversion system. A fundamental titanium (Ti):sapphire laser at 770 nm (1.61 eV) with an average power 600 mW and a repetition rate of 100 MHz was used to produce second harmonics (SH) at 385 nm (3.22 eV) with an average power of 10 mW in a 3-mm LBO crystal (type I). The SH was used to excite the samples after the separation from the fundamental by a dichroic mirror. The polarization of the excitation light was set parallel to the long axis of the molecule in the crystal. The average excitation power was less than 1 mW. The remaining fundamental was used as a probe beam to up-convert the fluorescence from the sample in a 0.5-mm BBO crystal (type I) by angle tuning. Thus, the polarizations of the probed fluorescence and the excitation pulse are parallel. The cross correlation between the SH and the fundamental had a full width at half-maximum of 260 fs when an objective lens was used for collecting the fluorescence. The measured cross correlation was chosen as a response function of the system. The up-converted signal was detected by a photomultiplier with a photon-counting system after passing through a monochromator. A continuous liquid N_2 flow cryostat was used to measure the fluorescence decay at 77 K.

III. Results

Stationary Fluorescence and Excitation Spectra. The stationary fluorescence and excitation spectra of the samples were measured at various temperatures to clarify the electronic structures of the samples. The absorption spectra of all samples could not be measured, since it was not possible to prepare a crystal thin enough to be used for the measurement of the absorption spectrum.

TABLE 1: Energy Parameters (eV) in ClSA, MClSA, and MSA[a]

	$E(S_1) - E(S_0)$	$E(S'_1) - E(S'_0)$	$E(S_0) - E(S'_0)$	$E(S_1) - E(S'_1)$
ClSA	2.496	2.421	0.031	0.044
MClSA	2.637	2.507	0.100	0.030
MSA	2.570	2.479	0.068	0.023

[a] $E(S_n)$ is the energy of the S_n state.

Figure 1 shows the fluorescence excited at 3.10 eV and excitation spectra probed at 2.18 eV at various temperatures of MClSA. The excitation spectra did not depend on the probed fluorescence energy. The fluorescence and excitation spectra of ClSA and MSA were similar to those of MClSA. Compared with the absorption and fluorescence spectra in solution, no prominent structures, which are expected to be originated from excitonic effects in crystal, were observed. Two common features of the thermochromic SAs were observed: One is that the absorption of the thermochromic band around 2.4 eV in the excitation spectra increased with temperature above 70 K, indicating that the keto form is thermally populated. The other is that the large Stokes shift of the fluorescence was observed below 70 K. Since the fluorescence band has a mirror symmetry with the thermochromic absorption band in the excitation spectrum and since the fluorescence could be observed by the selective excitation of the thermochromic absorption band, the stationary fluorescence originates mainly from the keto form. Thus, the large Stokes shift of the fluorescence below 70 K shows that the excited enol form relaxes to the excited keto form, indicating that the photoexcitation causes the proton transfer.

Using the excitation and fluorescence spectra, the energy separations between the states, S_1 and S_0 (E_e), S'_1 and S'_0 (E_k), and S_0 and S'_0 (E_a), are estimated experimentally. The values of E_e and E_k were estimated from the lowest edges of the excitation spectra and the highest edges of the fluorescence spectra, respectively, at the lowest temperature to eliminate the thermal effects. In the present study, the edge of each spectrum is defined as the photon energy where the intensity becomes 1/20th of the peak intensity in each spectrum to remove the ambiguity. The value of E_a was evaluated from the temperature dependence of the thermochromic band in the excitation spectrum by assuming the Boltzmann distribution of the population of the keto form. As a result, the energy separation between S_1 and S'_1 (E_g) was obtained. The results are listed in Table 1. The value of E_g was found to reduce in the order of ClSA, MClSA, and MSA, which is correlated with the dynamics of the proton transfer, as will be discussed later.

Time-Resolved Fluorescence. (1) Time-Resolved Fluorescence. Parts a, b, and c of Figure 2 show the time dependence of the fluorescence intensities of ClSA, MClSA, and MSA, respectively, at the probe photon energies at room temperature.

In ClSA, the kinetics of the fluorescence is strongly dependent on the probe photon energy. On the higher energy side of the fluorescence spectrum, the rapid fluorescence decay is observed, while the fluorescence decays relatively slowly on the lower energy side. In the intermediate region, the decay function is biexponential with the lifetimes of subpicoseconds and several hundred picoseconds with varying fractions depending on the photon energy, indicating the existence of two fluorescent species. The solid lines in Figure 2a represent the fitted curves by the least-squares method with the response function convoluted. The decay rate of the fast decay component was

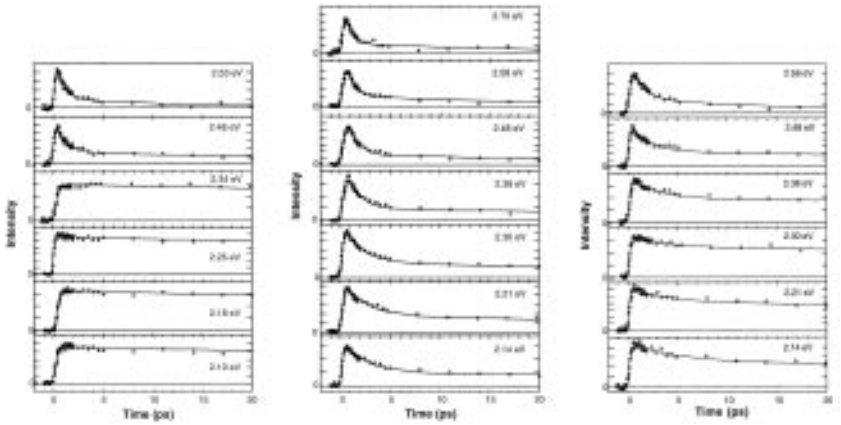

Figure 2. (a, left) Fluorescence decay at 2.53, 2.48, 2.34, 2.25, 2.18, and 2.10 eV excited at 3.22 eV of ClSA at 293 K from the top to the bottom. (b, middle) Fluorescence decay at 2.70, 2.58, 2.48, 2.38, 2.30, 2.21, and 2.14 eV excited at 3.22 eV of MClSA at 293 K from the top to the bottom. (c, right) Fluorescence decay at 2.58, 2.48, 2.38, 2.30, 2.21, and 2.14 eV excited at 3.22 eV of MSA at 293 K from the top to the bottom.

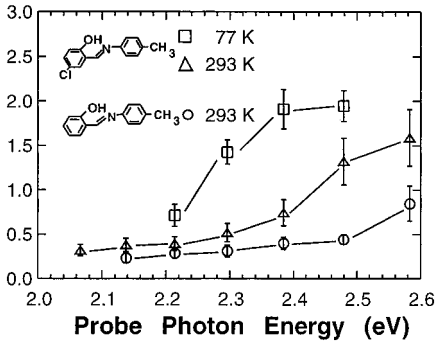

Figure 3. Probe photon energy dependence of the fast decay rate of the fluorescence from MClSA at 293 K (open squares) and 77 K (open triangles) and from MSA at 293 K (open circles).

determined to be 1.28 ± 0.04 ps^{-1}. Since the time-integrated intensity of the slow decay component was about 500 times larger than that of the fast decay component and since the slow decay component was observed in the same region of the stationary fluorescence spectrum, the slow decay component contributes dominantly to the stationary fluorescence spectrum. Hence, the slow decay component is attributed to the fluorescence of the excited keto form. The origin of the fast decay component will be discussed later.

The fluorescence dynamics of the deuterated (ClSA-d) species, in which the hydrogen of interest is replaced by a deuterium atom, was also investigated to gain insight into the potential shape in the excited state. A similar time dependence was observed. However, the decay rate of the fast decay component was 1.00 ± 0.04 ps^{-1}, which is smaller than that of ClSA. The deuteration effect was observed.

The bimodal fluorescence decays in MClSA and MSA were also fitted by the biexponential function with decay times of subpicoseconds and several hundred picoseconds. The results are shown by the solid curves in parts b and c of Figures 2. Since the time-integrated fluorescence intensity of the slow decay component is dominant, the slow decay component is also ascribed to the fluorescence of the excited keto form, as in the case of ClSA. However, the fluorescence kinetics was different from that of ClSA in the following point: The fast decay rate becomes larger at the higher probed photon energy from 0.31 to 1.6 ps^{-1} in MClSA and from 0.23 to 0.85 ps^{-1} in MSA. Figure 3 shows that the fast decay rate strongly depends on the fluorescence photon energy. At the lower energies, the decay rate becomes nearly constant at 0.36 ± 0.04 and at 0.28 ± 0.06 ps^{-1} in MClSA and in MSA, respectively. The decay rate of MClSA was faster than that of MSA at all probe photon energies. These differences among the three samples may be attributed to substitution effects.

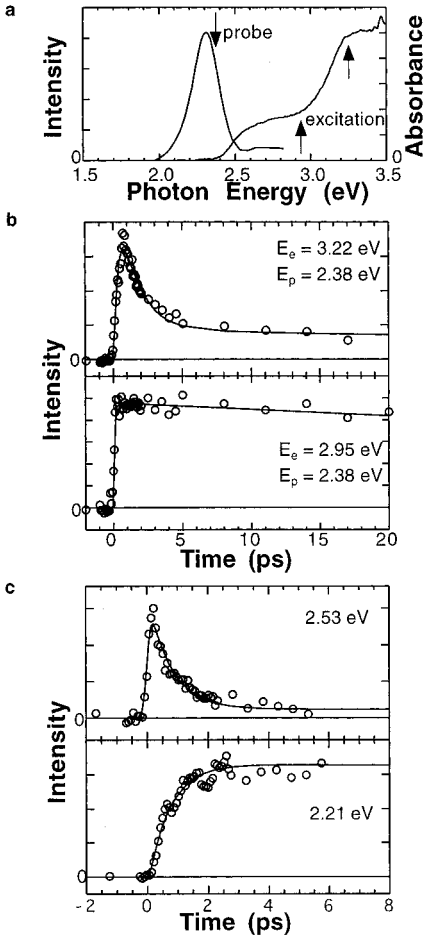

Figure 4. (a) Absorption and fluorescence spectra of MClSA 293 K. (b) Fluorescence decays of MClSA at 2.38 eV excited at 3.22 eV (upper) and 2.95 eV (lower) at 293 K. (c) Time dependence of the fluorescence of ClSA at 77 K. The fluorescence energies are 2.53 (upper) and 2.21 eV (lower).

(2) Selective Excitation of the Keto Form. In order to clarify the origin of the fast decay components of the present systems, MClSA was also excited at 2.95 eV by tuning the Ti: sapphire laser: The keto form is excited more efficiently than the enol form as shown in the absorption spectrum of Figure 4a, in which the absorption band between 2.5 and 2.9 eV is the thermochromic band.

Parts b and c of Figure 4 show that the dynamics of the fluorescence decay at 2.38 eV strongly depends on the excitation energy; no fast decay components were observed when the thermochromic absorption band was excited efficiently at 2.95 eV, as shown in the lower part of Figure 4b. On the other hand, the bimodal fluorescence decay was observed when MClSA was excited at 3.22 eV, as shown in the upper part of Figure 4b. This indicates that the fast decay corresponds to the relaxation of the excited enol form.

Compared with the absorption spectrum, the absorbance in the excitation spectrum at 297 K increases with the photon energy at 3.3 eV. This may be due to the difference in the experimental conditions. Powderlike samples made of many small crystals were used for the measurement of the excitation spectra. The excitation spectrum does not agree with the absorption spectrum of the sample of larger size. The efficiency of the excitation is reduced because of the strong scattering of the excitation light at shorter wavelengths. The light intensity from the Xe lamp strongly depends on the photon energy between 2.5 and 3 eV, and it becomes lower rapidly beyond 3 eV, which makes it difficult to obtain the correct excitation spectrum. Thus, it is difficult to compare the absorbance of the enol form and that of the keto form using the excitation spectrum, although it is enough to identify the enol and keto forms in the excitation spectrum.

(3) Low-Temperature Measurement. The fluorescence dynamics of ClSA and MClSA were investigated at 77 K to gain insight into the process of the proton transfer. Since the keto form is thermally populated at room temperature, it is difficult to observe the rise time of the fluorescence of the keto form. On the other hand, the evolution of the fluorescence of the keto form is expected to be observed at 77 K. The time dependence of the fluorescence of ClSA at 77 K at 2.53 and 2.21 eV is shown in Figure 4c. The lifetime at 2.53 eV was 0.76 ± 0.05 ps, which agrees with the rise time of 0.72 ± 0.05 ps at 2.21 eV. This agreement strongly suggests that the fast decay component is the precursor to the slow component. In MClSA, the fluorescence also decays biexponentially, similar to the measurements at 293 K. The fast decay rate at the probe photon energy of MClSA is also plotted in Figure 3.

IV. Discussion

Dynamics of Proton Transfer. From the femtosecond fluorescence spectroscopy, the lifetime of the excited enol state was found to be less than a few picoseconds. In addition to the proton transfer, three other possible decay mechanisms of the excited enol state can be considered: (1) intersystem crossing to a triplet state and (2) radiative and (3) nonradiative decays to the ground enol state. Since the radiative lifetime of the excited state of an organic molecule is generally a few nanoseconds, the second mechanism can be ruled out. In addition, the time of singlet−triplet intersystem crossing of an aromatic compound is longer than several hundred picoseconds.[37] Hence, the first mechanism does not contribute dominantly to the decay of the excited enol state. If the nonradiative decay to the ground enol state is the main pathway, the sample would hardly fluoresce. On the other hand, the three samples are highly fluorescent. Therefore, it can be concluded that the third mechanism is much less important than the proton transfer in the present system and that the decay rate of the excited enol state almost corresponds to the proton-transfer rate.

Consequently, the rate of the proton transfer in ClSA is determined to be 1.28 ± 0.04 ps^{-1}. In MClSA and MSA, the decay rate of the fluorescence of the enol form becomes constant at the lower fluorescence energy, as shown in Figure 3. Since the observed decay rate is much higher than those of the radiative decay and the intersystem crossing, the almost constant decay rate at the lower energy is considered to be due to the proton transfer from S_1 to S'_1. Thus, the rates of the proton transfer in MClSA and MSA are determined to be 0.36 ± 0.04 and 0.28 ± 0.06 ps^{-1}, respectively. Two decay components at lower fluorescence energies suggest the existence of the potential barrier between the excited enol and keto forms: If there were no barriers, the fluorescence would decay exponentially with the continuous elongation of the decay time from the higher to lower energies in a fluorescence spectrum. In addition, the rate of proton transfer should be much larger in the barrierless potential as observed in 2-(2′-hydroxy-5′-methylphenyl)benzotriazole (TIN)[6,8,9] and 3-hydroxyflavone,[11] in which the rate of proton transfer is 6.7 and 4.2 ps^{-1}, respectively. These proton-transfer rates are considered to be determined by the frequency of the vibrational mode involving the hydrogen bond.[6,8,9]

The low-temperature experiment offers information to clarify the mechanism of the proton transfer. At 77 K, the rate of proton transfer was not much different from that at room temperature. Since the rate of proton transfer by the thermal activation mechanism is expected to become exponentially lower with temperature, it is concluded that quantum-mechanical proton tunneling through the barrier is taking place.

The existence of the barrier is supported by the deuteration effect on the dynamics of the proton transfer; the rate of proton transfer in ClSA becomes smaller by deuteration from 1.28 to 1.00 ps^{-1}. In the potential with a barrier, the rate of proton transfer correlates with the frequency of the O−H stretching mode. Thus, the reduction of the rate by deuteration indicates the existence of the barrier. This contrasts with the previous results of the proton transfer in the femtosecond region,[9,15] which might be due to the difference in phase of the investigated system: In the liquid or gas phase, a molecule can be more deformed to shorten the hydrogen-bond length for lack of intermolecular interactions, resulting in the barrierless potential. It is, however, necessary to investigate the potential shape of the proton transfer further.

In MClSA and MSA, the decay rate of the fluorescence of the enol form was found to be smaller at the lower fluorescence energy. Two fluorescence processes can be tentatively considered to be the origin of the change in the decay rate of the fluorescence: (1) the fluorescence of the nonthermally excited S_1 vibrational levels and (2) the fluorescence of the higher energy states (S_n). In the first process, the probe energy dependence of the fast decay rate is due to the repopulation among the S_1 vibrational levels: Since the present molecular system was excited with an excess energy with respect to the S_1 state, the SA molecule is expected to be in a vibrationally nonthermalized state after the femtosecond pulse excitation. The nonthermally vibrational distribution makes it possible to emit fluorescence with higher energy. The fluorescence decay rate is determined by the rate of thermalization of a molecule and is expected to depend on the probed fluorescence energy: The decay rate becomes smaller in the lower energy region of the fluorescence spectrum. In the second process, the decay rate is determined by the rate of internal conversion. Thus, the decay rate of the short-wavelength fluorescence is larger.

The present experimental result can be attributed not to process 2 but to process 1 for the following two reasons: Firstly, the fast decay component was observed below the absorption edge of the enol form determined by the stationary excitation spectra at 10 K. This suggests that the fluorescence is emitted from S_1; the fluorescence from S_n is expected to be observed even above the absorption edge of the enol form. Secondly,

the observed decay rate is much lower than that expected for the internal conversion: In MSA, the shortest decay time of the fluorescence observed is 1.2 ps, which is too long to be an internal conversion time between the excited states with the same spin manifold.[38] On the other hand, the observed decay rate is reasonable as the rate of thermalization. In the present system, the thermalization process is considered to be competing with the proton transfer, 0.36 and 0.28 ps^{-1} in MClSA and MSA, respectively. These rates are consistent with the rate of thermalization, 0.2 ps^{-1}, estimated in TIN.[13] In another large aromatic molecule, α-terthiophene, it was also found that the intramolecular vibrational population redistribution occurs in a few picoseconds.[39]

Therefore, the fluorescence kinetics in the present SAs can be considered as follows: Photoexcitation transfers the enol form to the vibrationally excited S_1 states via vertical transition. The vibrationally hot states thermalize within a few picoseconds. At the same time, the proton is transferred to the excited keto state with the rates of 1.28, 0.36, and 0.28 ps^{-1} in ClSA, MClSA, and MSA, respectively, and then the molecules relax to the ground state. Here, since the energy separation between the excited enol (S_1) and keto states (S'_1) is less than 0.04 eV, the thermally populated excited enol state is expected at higher temperatures after the proton transfer. Thus, strictly speaking, the decay rate of the slow component corresponds to the weighted average of the relaxation rates of the S_1 and S_1' states at room temperature.

Substitution Effects. The following two prominent changes in the fluorescence dynamics were observed by substitution: (1) The rate of the proton transfer becomes smaller in the order of ClSA, MClSA, and MSA. (2) The decay rate of the fluorescence of the enol form becomes smaller at the lower fluorescence energies in MClSA and MSA, although it was not observed in ClSA.

The difference in the dynamics of the proton transfer among ClSA, MClSA, and MSA can be explained in terms of the change in the barrier height of the potential-energy surface in the excited state. The energy separation (E_g) between the excited enol (S_1) and keto (S'_1) forms is obtained from the results of the stationary fluorescence and excitation spectra as listed in Table 1. The values of E_g of ClSA, MClSA, and MSA are 44, 30, and 23 meV, respectively, while the proton-transfer rates in ClSA, MClSA, and MSA are 1.28, 0.36, and 0.28 ps^{-1}, respectively. If it is assumed that the hydrogen-bond lengths are not different among the three systems, both the height and thickness of the potential barrier increase with a decrease in E_g, resulting in the lower probability of the proton tunneling. Hence, the rate of proton transfer becomes lower with a decreasing E_g.

In the case of ClSA, the thermalization process was not observed. This is because the rate of proton transfer, 1.28 ps^{-1}, is much higher than that of the thermalization, 0.2 ps^{-1}: The proton transfer finishes before the thermalization. The absence of the thermalization in ClSA is also attributed to the lower barrier height of the potential in the excited state.

The difference in E_g among the samples may be ascribed to the substitution effect as follows: Since the chlorine atom attracts the electrons of the oxygen atom through the σ bond by the inductive effect, it decreases the strength of the O−H bond. Thus, the chlorination reduces the barrier height between the enol and keto forms. The methyl group is a π-electron donor. It enhances the proton-accepting property of the nitrogen atom forming the hydrogen bond, resulting in the lower barrier height. It is, however, difficult to predict which is more effective, the chlorine atom or the methyl group. Since E_g of ClSA is larger than that of MSA, it is considered that the chlorine atom stabilizes the keto form more efficiently in the present case.

The value of E_g in MClSA does not have the largest value among the three, indicating that the energy stabilization is not the simple summation of the chlorine and methyl substitution effects. This may be explained as follows: The chlorine atom also donates the π electron by the resonance effect; the wave functions of the π electrons from the chlorine atom may interfere with that of the methyl group, resulting in the reduction of the resonance effect of the methyl group. Thus, these two substituents cannot simply give additional effects.

V. Summary

The substitution effect on the dynamics of the proton transfer in the thermochromic SA in the crystalline phase was investigated using femtosecond time-resolved fluorescence spectroscopy. It is concluded that the proton transfer takes place by the quantum-mechanical tunneling in the excited state from the deuteration effect and the low-temperature experiment. The rate of proton transfer was found to increase in the order of MSA, MClSA, and ClSA, which can be explained by the different barrier heights of the potential in the excited state indicated by the stationary fluorescence and excitation spectra. The change in the potential is qualitatively explained by the electron-donating or -accepting property of the substituent around the hydrogen bond. In ClSA and MSA, the thermalization of the vibrationally hot states in S_1 was observed.

Acknowledgment. We are grateful to Profs. U. Nagashima and T. Mitani for valuable discussions. We thank Dr. K. Misawa and Ms. A. Yang for their technical support. The work was partly supported by a Grant-in-Aid for specially Promoted Research from the Ministry of Education, Science, and Culture (No. 0510200021).

References and Notes

(1) Shizuka, H.; Machii, M.; Higaki, Y.; Tanaka, M.; Tanaka, I. *J. Phys. Chem.* **1985**, *89*, 320 and references therein.
(2) Barbara, P. F.; Walsh, P. K.; Brus, L. E. *J. Phys. Chem.* **1989**, *93*, 29.
(3) Photoinduced proton transfer, Michael Kasha Festschrift; *J. Phys. Chem.* **1991**, *95*, 10215.
(4) Ultrashort Laser Pulses, 2nd ed. *Topics in Applied Physics*; Kaiser, W., Ed.; Springer: 1993; Vol. 60, Chapter 8, Addendum G, and references therein.
(5) Elsaesser, T.; Schmetzer, B.; Lipp, M.; Bauerle, R. J. *Chem. Phys. Lett.* **1988**, *148*, 112.
(6) Laermer, F.; Elsaesser, T.; Kaiser, W. *Chem. Phys. Lett.* **1988**, *148*, 119.
(7) Wiechmann, M.; Port, H.; Laermer, F.; Frey, W.; Elsaesser, T. *Chem. Phys. Lett.* **1990**, *165*, 28.
(8) Wiechmann, M.; Port, H.; Frey, W.; Laermer, F.; Elsaesser, T. *J. Phys. Chem.* **1991**, *95*, 1918.
(9) Frey, W.; Laermer, F.; Elsaesser, T. *J. Phys. Chem.* **1991**, *95*, 10391.
(10) Frey, W.; Elsaesser, T. *Chem. Phys. Lett.* **1992**, *189*, 565.
(11) Schwartz, B. J.; Peteanu, L. A.; Harris, C. B. *J. Phys. Chem.* **1992**, *96*, 3591.
(12) Arthen-Engeland, Th.; Bultmann, T.; Ernsting, N. P.; Rodriguez, M. A.; Thiel, W. *Chem. Phys.* **1992**, *163*, 43.
(13) Lenz, K.; Pfeiffer, M.; Lau, A.; Elsaesser, T. *Chem. Phys. Lett.* **1994**, *229*, 340.
(14) Chudoba, C.; Lutgen, S.; Jentzsch, T.; Riedle, E.; Woerner, M.; Elsaesser, T. *Chem. Phys. Lett.* **1995**, *240*, 35.
(15) Herek, J. L.; Pedersen, S.; Banares, L.; Zewail, A. H. *J. Chem. Phys.* **1992**, *97*, 9046.
(16) Barbara, P. F.; Rentzepis, P. M.; Brus, L. E. *J. Am. Chem. Soc.* **1980**, *102*, 2786.
(17) Kobayashi, T.; Dengenkolb, E. O.; Rentzepis, P. M. *J. Phys. Chem.* **1979**, *83*, 2431.
(18) Flom, S.; Barbara, P. F. *Chem. Phys. Lett.* **1983**, *94*, 488.
(19) Strandjord, A. J. G.; Barbara, P. F. *J. Phys. Chem.* **1985**, *89*, 2355.
(20) Dick, B.; Ernsting, N. P. *J. Phys. Chem.* **1987**, *91*, 4261.

(21) Cohen, M. D.; Schmidt, G. M. J. *J. Phys. Chem.* **1962**, *66*, 2442.
(22) Cohen, M. D.; Schmidt, G. M. J.; Flavian, S. *J. Chem. Soc*. **1964**, 2041.
(23) Bregman, J.; Leiserowitz, L.; Schmidt, M. J. *J. Chem. Soc*. **1964**, 2068.
(24) Bregman, J.; Leiserowitz, L.; Osaki, K. *J. Chem. Soc*. **1964**, 2086.
(25) Cohen, M. D.; Flavian, S.; Leiserowitz, L. *J. Chem. Soc. B* **1967**, 329.
(26) Cohen, M. D.; Flavian, S. *J. Chem. Soc. B* **1967**, 334.
(27) Hadjous, E.; Milia, F.; Seliger, J.; Blinc, R.; Zagar, V. *Chem. Phys.* **1980**, *47*, 105.
(28) Hadjous, E. *J. Photochem.* **1981**, *17*, 355.
(29) Hadjous, E. *Mol. Eng.* **1995**, *5*, 301.
(30) Richey, W. F.; Becker, R. S. *J. Chem. Phys.* **1968**, *49*, 2092.
(31) Nakagaki, R.; Kobayashi, T.; Nakamura, J.; Nagakura, S. *Bull. Chem. Soc. Jpn*. **1977**, *50*, 1909.
(32) Lewis, J. W.; Sandorfy, C. *Can. J. Chem.* **1982**, *60*, 1738.
(33) Becker, R. S.; Lenoble, C.; Zein, A. *J. Phys. Chem.* **1987**, *91*, 3509.
(34) Turbeville, W.; Dutta, P. K. *J. Phys. Chem.* **1990**, *94*, 4060.
(35) Yuzawa, T.; Takahashi, H.; Hamaguchi, H. *Chem. Phys. Lett.* **1993**, *202*, 221.
(36) Shah, J. *IEEE J. Quantum Electron.* **1988**, *24*, 276.
(37) Wilkinson, F. In *Organic Molecular Photophysics;* Birk, J. B., Ed.; John Wiley & Sons: New York, 1975; Vol. 2, Chapter 3.
(38) Swenberg, C. E.; Geacitov, N. E. In *Organic Molecular Photophysics*; Birk, J. B., Ed.; John Wiley & Sons: New York, 1973; Vol. 1, Chapter 10.
(39) Yamaguchi, S.; Hamaguchi, H. *Chem. Phys. Lett.* **1994**, *227*, 255.